Prediction of the Cutting Forces and Chip Morphology When Machining the Ti6Al4V Alloy Using a Microstructural Coupled Model

D. Yameogo, B. Haddag, H. Makich, Mohammed Nouari

Available online at www.sciencedirect.com

ScienceDirect

Procedia CIRP 58 (2017) 335 – 340

www.elsevier.com/locate/procedia

16th CIRP Conference on Modelling of Machining Operations

Prediction of the cutting forces and chip morphology when machining the Ti6Al4V alloy using a microstructural coupled model

D. Yameogo*, B. Haddag, H.Makich, M. Nouari*

University of Lorraine, Laboratoire d'Energétique et de Mécanique Théorique et Appliquée, LEMTA CNRS-UMR 7563, Mines Albi, Mines Nancy, GIP-InSIC, 27 rue d'Hellieule, 88100 Saint-Dié-des-Vosges, France

* Corresponding authors. Tel.: +33 (0)3 29 42 18; fax: +33 (0)3 29 42 18 25. *E-mail address:* yameogo1@univ-lorraine.fr, mohammed.nouari@univ-lorraine.fr

Abstract

Titanium and its alloys are often used in aerospace, power and biomedical applications due to their low density, high tensile strength, resistance to corrosion and high temperatures. However, these materials are well known to be difficult-to-cut materials and require to follow some special techniques to improve their machinability. It should be also noticed that some phenomena like segmentation and recrystallization can occur during the chip formation process. Therefore, fine grains are observed in the adiabatic shear bands located in the chip segments. The machined surface also presents fine grains because of the recrystallization of the microstructure. In the present work, a 2D finite element model based on Lagrangian formulation was developed in Abaqus/Explicit to simulate the orthogonal cutting process of the Ti6Al4V alloy. To take into account the recrystallization phenomenon, a new material constitutive model denoted 'Multi-Branch Model' (MB) was developed. The MB model is based on the Johnson-Cook (JC) flow stress model and its modified formulation, known as the tangent hyperbolic model (TANH), to introduce the softening effect due to the recrystallization process. This new model is coupled to a microstructural criterion in order to simulate the work-material microstructure evolution during the machining process. The recrystallized grains size field, cutting forces and chips morphology are compared to those obtained with the TANH model. Based on these results, a relationship between recrystallization and chip segmentation has been found and deeply discussed.

Peer-review under responsibility of the scientific committee of The 16th CIRP Conference on Modelling of Machining Operations

Keywords: Keywords: Metal machining; Titanium Alloy; Microstructure; Recrystallization; Grain size; FE Modelling

Nomenclature

A	Initial yield stress (MPa)
B	Hardening modulus (MPa)
C	Strain rate dependency coefficient
d_0	Initial grain size
d_{DRX}	Recrystallized grain size
m	Thermal softening coefficient
n	Strain hardening coefficient
Q_{act}	Dynamic recrystallization activation energy (J)
R	Boltzmann constant
T	Temperature (°K)
T_0	Reference Temperature (°K)
T_m	Melting Temperature (°K)
ε	Equivalent plastic strain
$\dot{\varepsilon}$	Equivalent plastic strain rate
ε_{crit}	Critical equivalent plastic strain
σ_{JC}	JC model Flow stress (MPa)
σ_{TANH}	TANH model Flow stress (MPa)
σ_{MB}	MB model Flow stress (MPa)
a_1, h_1, m_1, c_1, a_2, a_8, h_8, m_8, c_8	JMAK model constants
a, b, c, d	JC model constants

Peer-review under responsibility of the scientific committee of The 16th CIRP Conference on Modelling of Machining Operations
doi:10.1016/j.procir.2017.03.233

1. Introduction

Titanium and its alloys are used in several industrial applications because of their interesting thermomechanical properties. Their resistance under high temperatures makes them more appropriate to design aeronautical engine parts. Also, they are very helpful for biomedical applications (e.g. fabrication of prosthesis) because of their low reaction with biological substances.

However, titanium alloys are considered as difficult-to-cut materials for which several microstructural phenomena can occur during the machining process.

The analysis of the microstructural evolution during the machining of these materials can help to better understand these phenomena and hence find new solutions to improve their machinability.

In this paper, the machining of the Ti6Al4V alloy, often used in aeronautic applications, was studied. Segmented chips are frequently generated and microstructure change occurs in the localized shear bands during the chip formation process. Several authors have studied the formation of such chips morphology. Kouadri et al. [1] proposed two parameters to quantify segmented chip morphology. Ma et al. [2] studied the mechanism of segmented chip formation experimentally and numerically for Ti6Al4V alloy. Hua and Shivpuri [3] used a finite elements model with a Lagrangian formulation to analyze segmentation process of Ti6Al4V alloy. Miguelez et al. [4] studied the influence of cutting speed and feed rate on segmentation using an orthogonal cutting model.

Segmented chips are generally explained by two main mechanisms: fracture and thermoviscoplastic deformation.

The first mechanism used to explain serrated chips is fracture. An example of crack due to fracture mechanism is shown in Fig.1a. Shaw and Vyas [5] explained this by cyclic fracture mechanism which is the raison of the chip segmentation. Umbrello [6] used a Cockroft and Latham's criterion to predict the segmented chip formation in a 2D simulation with DEFORM-2D software. A periodic crack initiation and propagation simulated by an element deletion feature are used. Aurich and Bil [7] used DEFORM-3D to study the formation of a chip due to fracture.

The second mechanism is the localized thermoviscoplastic deformation, characterized by the formation of Adiabatic Shear Band (ASB), Fig.1b. Different interpretations were given in Literature to this shear strain localization. Wan et al. [8] explained that the thermoplastic instability is due to the shift between the heat flux and the plastic strain rate. They observed the ASB formation process for the Ti6Al4V alloy. According to their analysis, the low thermal conductivity leads to a localized catastrophic failure of the material and then to the formation of the ASB. Aurich and Bil [7] also studied chip segmentation due to this thermoplastic instability which is attributed to the thermal softening. They modelled this phenomenon using Rhim's material model. They recalled that this thermal softening is often accompanied by dynamic recrystallization (DRX). Atmani et al. [9] [10] studied the microstructural change in metals during machining and used a multi-physics based modelling to simulate recrystallized grains during machining the OFHC copper. The Mechanical

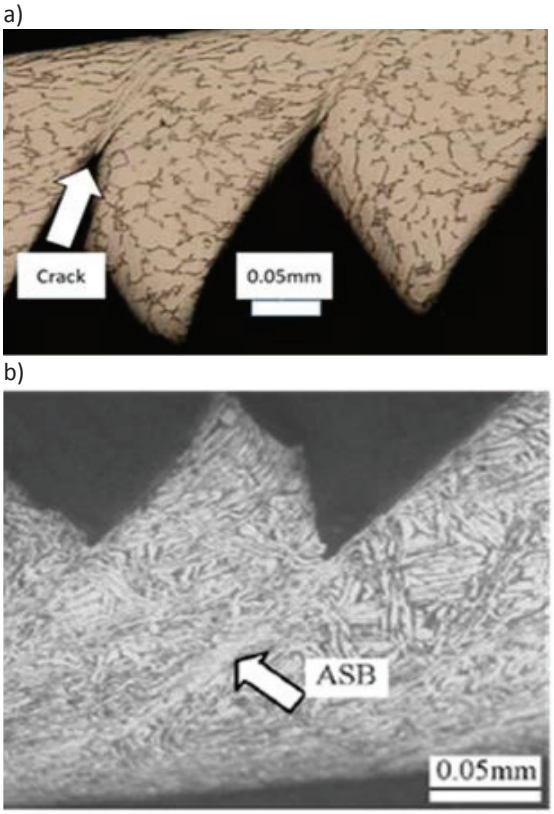

Fig. 1. Ti6Al4V serrated chip with cracks and ASB (a), Ti6Al4V serrated chip with ASB (b) [1].

Threshold Stress model (MTS) was used to describe the flow stress evolution and the dislocation density (DD) based model was used to obtain the microstructural evolution. When machining Ti6Al4V, recrystallized grains have been observed within the ASB. Nouari and Makich [11] point out the microstructural change in ASB while studying both titanium alloys Ti6Al4V and Ti-555. Wan et al. also noticed this fact [8]. Calamaz et al. [12] linked the recrystallization with a "strain softening phenomenon" by modifying the Johnson-Cook (JC) thermoviscoplastic model with a tangent hyperbolic function. The obtained behavior model, known as the Tangent Hyperbolic model (TANH), permitted to simulate serrated chips. It has been used later by several authors, like Sima and Ozel [13] or Ducobu et al. [14]. The TANH model generally predicts a good morphology of the chip. However it conducts to an overestimated segmentation frequency and lowers the amount of cutting forces [14],[15]. In this work, based on experimental observations [11], the assumption made is that the severe softening observed in ASB, only occurs when the material is subjected to dynamic recrystallization. Using a TANH model in all the chip body induces a lowering of the material rigidity and then a lowering of cutting forces. This is also the cause of the overestimation of the segmentation frequency. The new proposed Multi-Branch (MB) model takes into account the DRX triggering and changes in the material behavior. For this purpose, the well-known JC model, the

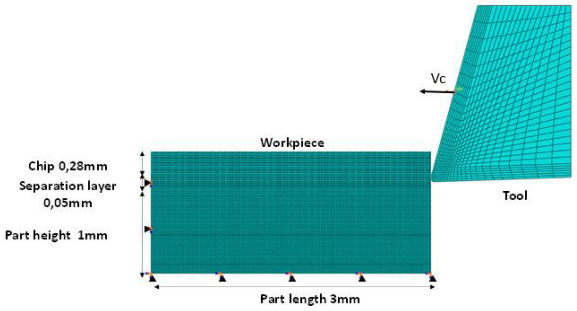

Fig. 2. Finite elements model of orthogonal cutting Ti6Al4V

TANH model, and the Johnson-Mehl-Avrami-Kolmogorov model (JMAK) have been used. The JC flow stress is applied to produce the behavior of the non-recrystallized areas, the TANH for the behavior of the recrystallized areas, and the JMAK model coupled with the flow stress is used to set the condition of recrystallization. The Finite Elements Software Abaqus/Explicit is used to implement the model and to simulate orthogonal cutting of Ti6Al4V alloy. A Lagrangian formulation was adopted. Two simulations are performed, one with the MB model and the other with the TANH model. The chip morphology and the cutting forces obtained from the two simulations are compared together. Finally, a discussion is conducted on the link between segmentation and recrystallization processes.

2. Proposed MB modelling

2.1. Machining tests parameters of the Ti6Al4V alloy

The proposed model in this work was validated by experimental data provided by Ducobu et al. [14]. A milling machine was used for the orthogonal cutting. The tool was fixed to the machine table and the part was mounted in the spindle and animated by a horizontal movement corresponding to the cutting speed. So there is no feed rate. The un-deformed chip thickness is called “depth of cut” because the current machining operation is not orthogonal turning. The part material is made of Ti6Al4V titanium alloy and the tool material of tungsten carbide. The tool geometry is characterized by a rake angle of 15°, clearance angle of 2° and an edge radius of 20µm. Cutting conditions are as follow: cutting speed is 30m/min, depth of cut is 0.28mm and width of cut is 1mm.

2.2. Finite element modelling

To predict the chip formation under orthogonal cutting configuration, a 2D finite elements model based on the Lagrangian formulation was performed with Abaqus/Explicit code. Two behavior laws for the work material were considered, the first one is the Multi-Branch behavior model and the second one is the TANH behavior model. The two behavior laws were implemented in Abaqus using the user material routine VUMAT.

In the FE model, the temperature is set at 25°C at the initial state. The tool is defined as a rigid body. The mechanical properties listed in Table 1 was taken from the work of Ducobu et al. [14]. The material flow stress models parameters listed in Table 2 are given in [14] and [16].
In the FE model, the workpiece is divided on three domains (see Fig.2): the un-deformed chip part, with dimension equal to the depth of cut (0.28mm), the separation layer which is used to form the chip using the element deletion technique, and the workpiece part which has a width of 1mm. The elements are deleted in the separation layer part when the damage reaches the value of 1. The Hillerborg’s failure criterion was used with the JC damage law. The equations and parameters of the failure criterion can be found in the work of Wang and Liu [17].

2.3. JC and TANH material behavior models

A thermoviscoplastic behavior model for machined metals is usually used in machining simulation, since the work material is subjected to high deformation and temperature. One of the most used behavior models is the JC flow stress model (1), written as follows:

$$\sigma_{JC} = \left(A + B\varepsilon^{n}\right)\left(1 + C\left[\ln\left(\frac{\dot{\varepsilon}}{\dot{\varepsilon}_0}\right)\right]\right)\left(1 - \left(\frac{T - T_0}{T_m - T_0}\right)^{m}\right) \tag{1}$$

Where ε is the plastic deformation, $\dot{\varepsilon}$ is the plastic deformation rate and T is the temperature. A, B, ε_0, T_0, T_m, n and m are material constants that need to be set.
The TANH model (Eq. (2)) presents a modification of the deformation hardening term in JC flow stress equation and another term is added with a TANH function:

$$\sigma_{TANH} = \left(A + B\varepsilon^{n}\left(\frac{1}{\exp\left(\varepsilon^{a}\right)}\right)\right)\left(1 + C\left[\ln\left(\frac{\dot{\varepsilon}}{\dot{\varepsilon}_0}\right)\right]\right)\left(1 - \left(\frac{T - T_0}{T_m - T_0}\right)^{m}\right)\left(D + (1 - D)\tanh\left(\frac{1}{(\varepsilon + S)^{c}}\right)\right) \tag{2}$$

with

$$D = 1 - \left(\frac{T}{T_m}\right)^{d} \quad \text{And} \quad S = \left(\frac{T}{T_m}\right)^{b}$$

where a, b, c and d are the material parameters. The last term of Eq. (2) with the TANH function brings to an intense softening of the material that has been called strain softening by Calamaz et al. [12]. The Fig.3 shows the influence of DRX and dynamic recovery on the strain-stress curve. This softening allows chip segmentation when simulating orthogonal cutting. However, this behavior is observed only when recrystallization occurs, and DRX only occurs within the ASB. Therefore, the material presents different behaviors depending on whether DRX occurs or not. This consideration brings to build a new behavior model for the chip formation of Ti6Al4V.

Table 1. Mechanical properties of the workpiece and tool materials[14]

	Ti6Al4V	Tungsten carbide
Density (kg/m3)	4430	15000
Young's modulus (GPa)	113.8	800
Expansion (K-1)	8.6e-6	4.7e-6
Conductivity (W/mK)	7.3	46
Specific Heat (J/ kg K)	580	203

2.4. The Multi-Branch model: MB model

As reported before, the orthogonal cutting simulations using the TANH model have a tendency to predict lower cutting forces and to overestimate the segmentation frequency. Based on these observations, two assumptions are made. The first assumption is to consider that the work material does not have the same behavior in the whole part, especially in the chip. A severe softening is observed only in certain areas, characterized by a severe plastic deformation. Due to this softening, the segmentation process occurs. Thus, a combination of two models, JC and TANH flow stress models is used to represent the material behavior. The second assumption is to associate the softening to DRX. This brings to consider that DRX is the cause of the softening. A criterion is defined to indicate when DRX occurs. This criterion is based on JMAK model and compares the plastic deformation to a critical deformation ε_{crit}. The equation (3) describes the calculation of the flow stress depending on the amount of the plastic deformation in comparison with the critical plastic deformation (Eq. (4)), [16].

$$\sigma_{MB} = \begin{cases} \sigma_{JC} \ if \ \varepsilon \le \varepsilon_{crit} \\ \sigma_{TANH} \ if \ \varepsilon > \varepsilon_{crit} \end{cases} \quad (3)$$

with σ_{JC} and σ_{TANH} given respectively by equations (1) and (2).

$$\text{with} \begin{cases} \varepsilon_{crit} = a_2 \, \varepsilon_{peak} \\ \varepsilon_{peak} = a_1 \, d_0^{h_1} \, \dot{\varepsilon}^{m_1} \exp\left(\frac{Q_{act} \, m_1}{R \, T}\right) + c_1 \end{cases} \quad (4)$$

In equation (4), d_0 is the initial grain size, Q_{act} the activation energy for DRX, R the Boltzmann constant, h_1, m_1 and c_1 are the model constants. The critical plastic deformation is calculated following an Arrhenius law. Therefore, this critical deformation decreases when the cutting temperature raises and increases when deformation rate raises. The DRX occurs when the plastic deformation is higher than the critical deformation and then the behavior of the material changes to TANH in order to soften. The Arrhenius law denotes the fact that recrystallization is a temperature activated phenomenon**.** Recrystallization occurs at higher plastic strain when strain rate increases. According to Quan et al. [18], the mobility of grain boundaries decreases when strain rate increases, which explains this phenomenon. This effect of strain rate on DRX onset is well described by the Arrhenius law. When there is not DRX, thermal softening, hardening and plastic rate hardening are represented with the JC flow stress model. The grain size is then calculated with the relationship (5), [16].

$$d_{DRX} = a_8 \, d_0^{h8} \, \dot{\varepsilon}^{m8} \exp\left(\frac{Q_{act} \, m_8}{R \, T}\right) + c_8 \quad (5)$$

Table 2. Models parameters[14] [16]

Parameters	MB	TANH
A (MPa)	968	968
B (MPa)	380	380
C	0.02	0.02
n	0.421	0.421
m	0.577	0.577
T_0 (K)	298	298
T_m (K)	1878	1878
a	1.6	1.6
b	0.4	0.4
c	6	6
d	0.5	0.5
a_1	2	2
h_1	0	0
m_1	0.006	0.006
c_1	0	0
a_2	0.38	0.38
a_8	15	15
m_8	-0.03	-0.03
c_8	0	0
d_0 (µm)	20	20
R (J K^{-1} mol^{-1})	8.31	8.31
Q_{act} (kJ mol^{-1})	218	218

Table 3. Morphology parameters comparison (χ : Average value, σ_χ : standard deviation).

Case	L (µm)		Fg (Hz)
	χ	σ_χ	
MB	195.5	4	2557
TANH	161	20	3098
Experimental[14]	206	17	2427

Table 4. Comparison of cutting forces mean values

Case	Cutting Force (N)	Feed Force (N)
MB	361	13.3
TANH	345	9.6
Experimental[14]	386	76

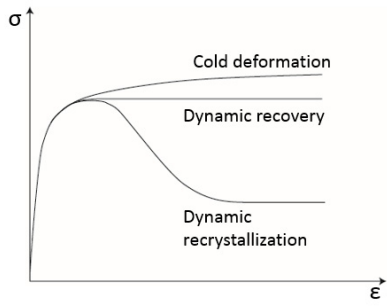

Fig. 3. Scheme of typical flow stress curves.

Equations (4) and (5) are also used to predict the grain size with the TANH model simulation.

3. Results and discussion

3.1. Chip morphology and grain size modification

The simulated and experimental chip morphologies have been compared through the segmentation frequency in Table 3. The segmentation frequency is calculated according to Ducobu et al. [14] by equation (5).

$$F_g = \frac{V_c}{L} \tag{5}$$

where F_g is the segmentation frequency, L the length defined in Fig. 4. V_c the cutting speed. The length L is measured on three segments for each model (TANH and MB). Irregular segments of the simulated chips have not been chosen as shown on Fig. 4. An average value is evaluated for each model and given in Table 3. The standard deviation of the MB model is lower than that of the TANH model. The MB model presents a lower segmentation frequency which is close to that found experimentally. The second investigated phenomenon is the microstructure change (average grain size distribution). Fig.4 shows the grain size in the chip. The ASB is characterized by high plastic deformation, but also by a fine grain size. The simulated ASB with MB model are more localized than that obtained with the TANH model. It is shown that the MB model predicts less number of segments than the TANH model because DRX only happens when certain conditions of plastic strain and temperature are reached. This triggering criterion is represented by the critical strain ε_{crit} .The chip segmentation process can be presented in three steps: In the first step, the load due to the tool induces the conditions of the recrystallization. This is the fact of the rapid increase and localization of temperature due to the low thermal conductivity of the Ti6Al4V alloy. The critical plastic deformation tends to decrease while temperature raises. Then, the recrystallization occurs when the plastic deformation is higher than the critical plastic deformation. The thermal softening facilitates this phenomenon. This means that the energy activation needed to trigger recrystallization has been reached. Finally, the

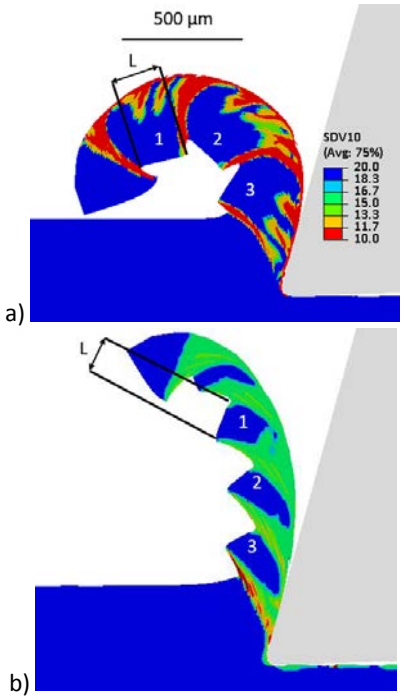

Fig. 4 Comparison of the grain size field and chip morphology of (a) MB model, and (b) TANH model.

recrystallization induces a severe softening in the region affected by recrystallization. This region of the chip undergoes the most plastic strain and the contrast with the non-affected areas of the chip appears. That contrast of plastic deformation appears to be the ASB and the segmentation phenomenon.

3.2. Cutting forces

The predicted and experimental cutting forces are reported in Table 4. The cutting forces predicted by the MB model are higher than the one obtained with the TANH model. The MB model is closer to the experimental result concerning this point. The feed force is very low for the two simulations in comparison with experimental data. This is due to the Lagrangian FE formulation used with elements deletion in the separated layers. It is well known that the elements deletion technique used to separate chip from the workpiece, affects predicted forces. Movaheddy [19] explained these disadvantages while introducing an ALE (Arbitrary Eulerian Lagrangian) approach. This problem of low feed force is observed in other papers using the same technique. Zhang et al. [20] compared different FE formulations: Lagrangian, ALE and CEL (Coupled Eulerian Lagrangian) to simulate Ti6Al4V chip formation. They predicted correctly the cutting force with the Lagrangian one (618N), while the measured one is 633N. However the feed force is largely underestimated (145N) in comparison to the measured one (559N). From Fig. 4, the recrystallized zone predicted with TANH model is larger than that obtained with the MB model. This indicates that the global rigidity of the chip is higher in the case of MB model than in the TANH model. The percentage of softened areas in the MB

model chip is smaller. Therefore, the chip shows more resistance toward the tool using the MB model. So a link can be established between the chip morphology and amount of cutting forces. Serrated chips are formed because of DRX, which induces a decrease of flow stress and then a decrease of cutting forces.

4. Conclusion

Two material behavior models have been considered in the framework of FE modelling of orthogonal cutting of the Ti6Al4V alloy. The first one is the TANH model, known to allow chip segmentation based on a strain softening. By considering that the DRX affects the behavior of the material and modifies the flow stress, a new model has been proposed with a criterion of DRX triggering. Thus, the resulted model (MB) was introduced to take into account the change of the flow stress curve depending on the DRX. In the region where DRX occurs the TANH flow stress law is activated and elsewhere the classical JC law is adopted. A better chip morphology, in terms of chip segmentation frequency, was obtained with the MB model. Also, higher values of cutting forces are obtained leading to a better prediction of experimental data. This is in accordance with the assumptions made previously. It suggests that DRX is responsible of chip morphology by softening some areas of the chip, creating a contrast of rigidity and therefore localizes plastic strain in softened areas (ASB). It allows a better prediction of cutting forces because it does not soften too much the material, but only where the DRX occurs.

References

[1] S. Kouadri, K. Necib, S. Atlati, B. Haddag, M. Nouari, Quantification of the chip segmentation in metal machining: Application to machining the aeronautical aluminium alloy AA2024-T351 with cemented carbide tools WC-Co, Int. J. Mach. Tools Manuf. 64 (2013) 102–113.

[2] W. Ma, X. Chen, F. Shuang, The chip-flow behaviors and formation mechanisms in the orthogonal cutting process of Ti6Al4V alloy, J. Mech. Phys. Solids. 98 (2017) 245–270.

[3] J. Hua, R. Shivpuri, Prediction of chip morphology and segmentation during the machining of titanium alloys, J. Mater. Process. Technol. 150 (2004) 124–133.

[4] M.H. Miguélez, X. Soldani, A. Molinari, Analysis of adiabatic shear banding in orthogonal cutting of Ti alloy, Int. J. Mech. Sci. 75 (2013) 212–222.

[5] M.C. Shaw, A. Vyas, Chip formation in the machining of hardened steel, CIRP Ann.-Manuf. Technol. 42 (1993) 29–33.

[6] D. Umbrello, Finite element simulation of conventional and high speed machining of Ti6Al4V alloy, J. Mater. Process. Technol. 196 (2008) 79–87.

[7] J.C. Aurich, H. Bil, 3D finite element modelling of segmented chip formation, CIRP Ann.-Manuf. Technol. 55 (2006) 47–50.

[8] Z.P. Wan, Y.E. Zhu, H.W. Liu, Y. Tang, Microstructure evolution of adiabatic shear bands and mechanisms of saw-tooth chip formation in machining Ti6Al4V, Mater. Sci. Eng. A. 531 (2012) 155–163.

[9] Z. Atmani, B. Haddag, M. Nouari, M. Zenasni, Combined microstructure-based flow stress and grain size evolution models for multi-physics modelling of metal machining, Int. J. Mech. Sci. 118 (2016) 77–90.

[10] Z. Atmani, B. Haddag, M. Nouari, M. Zenasni, Multi-physics modelling in machining OFHC copper–coupling of microstructure-based flow stress and grain refinement models, Procedia CIRP. 31 (2015) 545–550.

[11] M. Nouari, H. Makich, Experimental investigation on the effect of the material microstructure on tool wear when machining hard titanium alloys: Ti–6Al–4V and Ti-555, Int. J. Refract. Met. Hard Mater. 41 (2013) 259–269.

[12] M. Calamaz, D. Coupard, F. Girot, A new material model for 2D numerical simulation of serrated chip formation when machining titanium alloy Ti–6Al–4V, Int. J. Mach. Tools Manuf. 48 (2008) 275–288.

[13] M. Sima, T. Özel, Modified material constitutive models for serrated chip formation simulations and experimental validation in machining of titanium alloy Ti–6Al–4V, Int. J. Mach. Tools Manuf. 50 (2010) 943–960.

[14] F. Ducobu, E. Rivière-Lorphèvre, E. Filippi, Material constitutive model and chip separation criterion influence on the modeling of Ti6Al4V machining with experimental validation in strictly orthogonal cutting condition, Int. J. Mech. Sci. 107 (2016) 136–149.

[15] M. Calamaz, Approche expérimentale et numérique de l'usinage à sec de l'alliage aéronautique TA6V, Bordeaux 1, 2008.

[16] Y.M. Arısoy, T. Özel, Prediction of machining induced microstructure in Ti–6Al–4V alloy using 3-D FE-based simulations: Effects of tool micro-geometry, coating and cutting conditions, J. Mater. Process. Technol. 220 (2015) 1–26.

[17] B. Wang, Z. Liu, Shear localization sensitivity analysis for Johnson–Cook constitutive parameters on serrated chips in high speed machining of Ti6Al4V, Simul. Model. Pract. Theory. 55 (2015) 63–76.

[18] G. Quan, G. Luo, J. Liang, D. Wu, A. Mao, Q. Liu, Modelling for the dynamic recrystallization evolution of Ti–6Al–4V alloy in two-phase temperature range and a wide strain rate range, Comput. Mater. Sci. 97 (2015) 136–147.

[19] M. Movahhedy, M.S. Gadala, Y. Altintas, Simulation of the orthogonal metal cutting process using an arbitrary Lagrangian–Eulerian finite-element method, J. Mater. Process. Technol. 103 (2000) 267–275.

[20] Y. Zhang, J.C. Outeiro, T. Mabrouki, On the selection of Johnson-Cook constitutive model parameters for Ti-6Al-4V using three types of numerical models of orthogonal cutting, Procedia CIRP. 31 (2015) 112–117.